SECONDARY ELECTRON YIELD OF SRF MATERIALS

S. Aull*, CERN, Geneva, Switzerland and Universität Siegen, Germany
T. Junginger, H. Neupert, CERN, Geneva, Switzerland
J. Knobloch, Helmholtz-Zentrum Berlin and Universität Siegen, Germany

Abstract

The secondary electron yield (SEY) describes the number of electrons emitted to the vacuum per arriving electron at the surface. For a given geometry, the SEY is the defining factor for multipacting activity. In the quest of superconducting RF materials beyond bulk niobium, we studied the SEY of the currently most important candidates for future SRF applications: Nb_3Sn, NbTiN and MgB_2. All studies were done on clean but technical surfaces, i.e. on clean surfaces exposed to air and with their native oxides as it would be the case for SRF cavities.

INTRODUCTION

In the late 1970's multipacting was the main limitation for SRF cavities in terms of accelerating gradient. For multipacting to occur, free electrons need to be accelerated by the RF field, the emission and the arrival point have to meet certain symmetry criteria and the secondary electron yield (SEY) has to be greater than one [1]. Multipacting activity is suppressed as soon as one of the criteria is not fulfilled, which was achieved by optimizing the cavity geometry towards an elliptical shape. However, multipacting is still an issue for non-elliptical cavities, couplers and waveguides. The development of materials beyond niobium requires the evaluation of the secondary electron yield as a material parameter in order to avoid the return of multipacting as a performance limitation for elliptical cavities.

SECONDARY ELECTRON EMISSION

The SEY describes the number of (secondary) electrons emitted to the vacuum per arriving (primary) electron at the surface. Upon arrival the primary electron travels through the material elastically scattering with the lattice ions and inelastically scattering with electrons. The latter produce secondary electrons along the travelling path of the primary. With increasing incident energy the maximum penetration depth of the primary electron increases. Although secondary electrons are generated along the whole path the majority of secondaries is created at the end of the primary's path and the total number of secondary electrons increases with the energy of the primary electron. The secondaries diffuse into the material and get emitted if they reach the surface with a remaining energy high enough to overcome the surface-vacuum barrier [2]. The probability to escape decreases exponentially on a characteristic escape length. These two mechanisms define the typical bell shape of the SEY curve as function of primary electron energy: In the low energy regime more and more secondary electrons are produced and since they are produced close to the surface, they are likely to escape. For high primary energies, many secondary electrons are produced but they are less likely to reach the surface as they are produced deeper in the material. Both effects compensate each other leading to a maximum of the SEY curve when the penetration depth of the primary electron is comparable to the characteristic escape length. Is a SEY value reported for a given material or sample, it usually refers to this maximum.

SEY of Conductors and Insulators

The number of emitted electrons is given by the minimum energy to overcome the surface-vacuum barrier and the interaction of the secondaries with the material, i.e. the energy loss until reaching the surface. If an internal secondary electron passes through a metal, it mainly scatters on electrons in the conduction band which results in high energy loss. Once it reaches the surface it can only be emitted to the vacuum if its remaining energy exceeds the minimum escape energy which is the sum of the work function and the Fermi level and is in the order of 10 eV [3]. As a result, pure, oxide and contamination free metals have low secondary electron yields, ranging from 0.5 for lithium to 1.8 for platinum [3] while alloys range between 1.5 and 3. In contrast to metals, an internal secondary electron passing through an insulating material scatters with phonons and defects and might excite valence electrons into the conduction band if its energy is higher than the band gap. All three contributions are small compared to the scattering in metals so that the kinetic energy of many secondaries exceeds the electron affinity which is usually as low as 1 eV. As a consequence, many generated secondaries are emitted and insulators have typically SEY values $\gtrsim 4$.

MEASURING THE SEY

At CERN, there is a dedicated set-up for SEY measurements which is combined with an XPS[1] setup. This allows coupled SEY and XPS measurements at room temperature and without breaking the vacuum which results in altering the surface conditions. The SEY part is schematically shown in Figure 1 and a thorough description of the setup including a description of the electron gun and the vacuum system can be found in [4]. Primary electrons emitted from an electron gun with a certain energy bombard the sample under test. Secondary electrons as well as scattered primary electrons leave the sample surface and will be absorbed by the surrounding collector.Reemission from the collector is suppressed by positively biasing the collector. In order to

* sarah.aull@cern.ch

[1] X-ray photoelectron spectroscopy

ISBN 978-3-95450-178-6

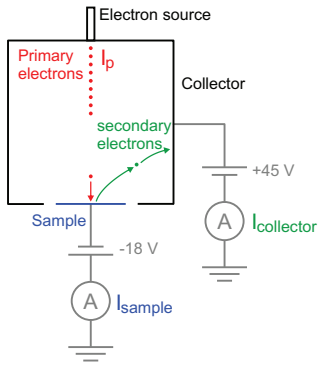

Figure 1: SEY setup at CERN. Biasing sample and collector suppresses re-absorption of secondary electrons by the sample surface.

calculate the SEY the current of the primary electrons I_p has to be known. The secondary electron yield can be derived from measuring the current on the sample I_{sample} and the collector current $I_{collector}$:

$$\text{SEY} = \frac{I_{collector}}{I_{sample} + I_{collector}} \quad (1)$$

All measurements are performed at room temperature, under vacuum ($< 10^{-8}$ mbar) and with a low primary electron dose ($< 10^{-6}$ C/mm^2).

Surface Preparation

The condition of the surface plays an important role for the secondary electron emission [5]. A high surface roughness decreases the SEY as the secondary electrons are more likely to be re-absorbed close to the emission site [2]. Moreover, the secondary electron emission is a process that takes place in the first few nanometers [6]. Therefore, adsorbed hydrocarbons and native oxides can have a great influence on the SEY. Literature SEY values refer usually to the bare material and were measured after removing any contamination and the oxide layer by sputtering or baking. SRF cavities are high pressure rinsed with ultra pure water and assembled in clean rooms. We are therefore mainly interested in the technical surface, i.e. a clean surface but exposed to air and with the native oxide layer. In order to have a reference, we prepared a RRR 300 bulk Nb sample with a bulk electropolishing to remove the damage layer from the production process as it is standard for SRF cavities. Moreover, a cavity is operated at liquid helium temperatures (≤ 4.5 K) so the residual gases from the vacuum will condense on the cavity surface. Although the room temperature measurement can not account for condensation of gases at cold it is known from experience with niobium cavities that this is not the defining factor for multipacting activity. As an example, TESLA shape cavities regularly exceed the multipacting band of 21 MV/m to 23 MV/m [7].

A NbTiN sample was coated onto a bulk Nb substrate at Jefferson Lab [8] and a Nb_3Sn sample was produced by reactive evaporation of tin into niobium at Cornell [9]. Both samples were packed under air for shipping. The niobium and the niobium alloy samples were degreased just prior to the SEY measurement. Two MgB_2 samples were deposited on SiC substrates at Temple University [10]. In order to protect the samples from humidity they were packed in (surface) contact free wafer boxes with packages of silica gel for shipping. As MgB_2 degrades under humidity, no further cleaning was done and the SEY was measured on the samples as received.

SEY OF SRF MATERIALS

The prepared surfaces can be assumed to be layered systems of the pure metals or alloys, different native oxides and a layer of hydrocarbon including water molecules embedded into the hydrocarbons [6]. The thickness of the latter strongly depends on the handling, time of air exposure, chemical treatment of the surface and heat treatment. Considering an oxide layer of a few nm and a contamination layer of comparable thickness the SEY will be strongly influenced by the surface condition and will be a superposition of the SEY values of the different components.

SEY of Bulk Nb

The SEY for the niobium reference sample was measured in three different spots to insure a uniform surface. As shown in Figure 2 there is no change across the sample surface. We find a maximum SEY of 2.2 which is in good agreement with previous SEY measurements on technical Nb [11] and significantly higher than the reported 1.3 for a clean Nb surface never exposed to air [12, 13]. The secondary electron yield of the niobium oxides NbO, NbO_2 and Nb_2O_5 were found to be lower than the one for pure niobium [13]. Also the SEY for pure niobium carbide powder and niobium nitride powder were found to be 0.8 if not exposed to air [13]. The SEY of water was estimated to 2.3 by condensing 200 monolayers of water molecules on a liquid nitrogen cooled surface [5].

Following the SEY measurement, we performed an XPS measurement to verify the chemical composition of the surface. The result is shown in Figure 3. Besides carbon, oxygen and niobium a small contamination with chromium was found which most likely came from tooling. Also clean metallic Cr is reported with a low SEY (1.1 [14]). The relatively high SEY can therefore be explained by the presence of hydrocarbons and water on the surface. Following the XPS, we sputter cleaned the surface until the carbon peak in the XPS spectrum disappeared. From the sputtering rate, a total removal of 3 to 5 nm was estimated. After the sputtering, the XPS data shows significantly less carbon and a reduction of niobium oxides. The reduction of niobium oxides is concluded from the shift of the niobium peaks in the XPS spectrum towards lower binding energies. The SEY measurement following the sputtering shows now a significant reduction of secondary electron emission and agrees well with the literature values for Nb and its native oxides.

ISBN 978-3-95450-178-6

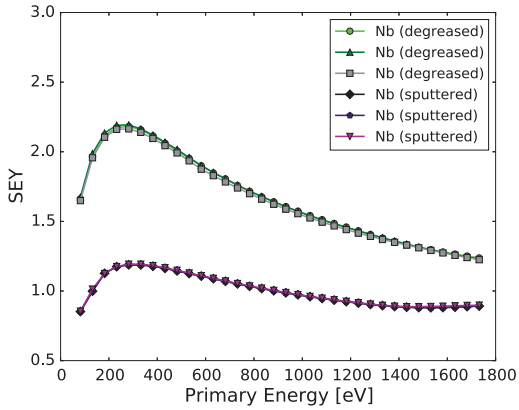

Figure 2: SEY of Nb measured at three different spots.

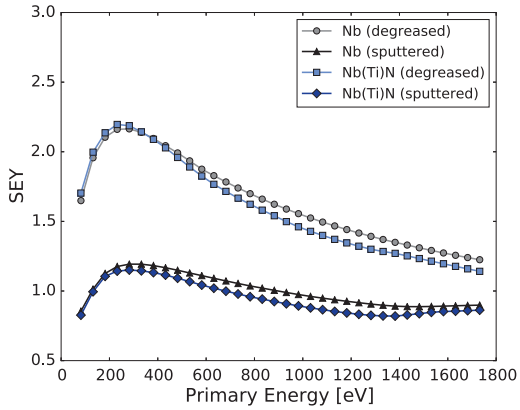

Figure 4: SEY of NbTiN

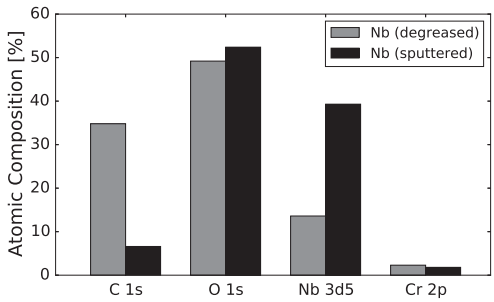

Figure 3: Chemical composition of the Nb surface based on the XPS measurements.

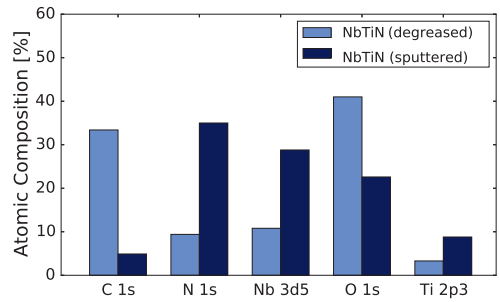

Figure 5: Chemical composition of the NbTiN surface based on the XPS measurements.

SEY of NbTiN and Nb_3Sn

The SEY and XPS measurements for the NbTiN and the Nb_3Sn sample were done in the same way as for the niobium sample: first the SEY was measured, then the sample was transferred to the XPS and measured. The same region was sputter cleaned and an XPS spectrum was measured again. Finally the SEY after sputtering was measured. In both cases, the SEY was measured in three spots across the surface. As for the Nb, the surfaces were very uniform so that in the following only one representative curve is shown. For better comparison, a representative data set of the Nb is shown as well.

Figure 4 and 5 show the results for the NbTiN sample. The XPS indicates hydrocarbons, the constituents of the film and oxygen but no other significant contamination. Before and after sputtering the sample exhibits the same SEY behaviour as the niobium sample which is consistent with SEY values around 1.2 for the sputtered surface, i.e. for the superposition of all present niobium compounds. Hydrocarbons and water can again explain the higher SEY of 2.2 before sputtering.

Figure 6 and 7 show the SEY and the according chemical composition of the Nb_3Sn surface. With a value of 2.4 the SEY of Nb_3Sn before sputtering is slightly higher than for the Nb and the NbTiN samples. Nb_3Sn is very resistant against oxidation [15]; however no SEY data is available on SnO_2 so the higher SEY might be due to this or another oxidation state on tin. After sputtering, the SEY is decreased to 1.3, comparable to Nb and NbTiN.

SEY of MgB_2

For both MgB_2 samples the SEY and the XPS spectra were measured. However, to avoid contamination of the vacuum chamber with boron, no sputter cleaning was done.

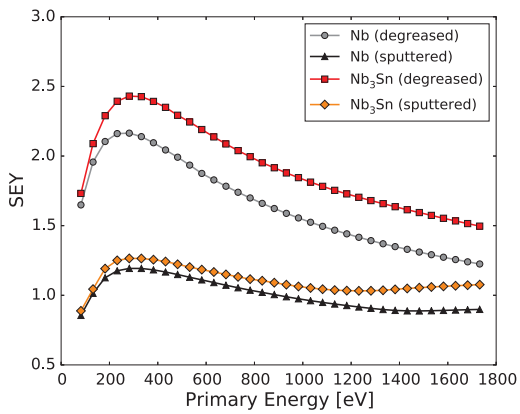

Figure 6: SEY of Nb_3Sn

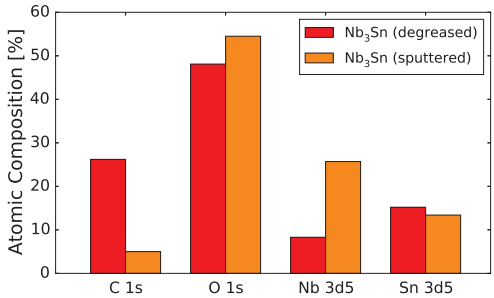

Figure 7: Chemical composition of the Nb_3Sn surface based on the XPS measurements.

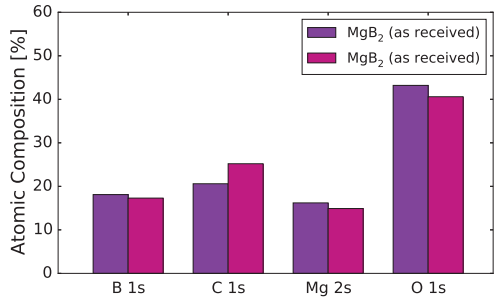

Figure 9: Chemical composition of the MgB_2 surfaces based on the XPS measurements.

Figure 8 shows the SEY measurements of both samples in comparison to niobium. As for the other samples, we measured three different spots across the surface which showed almost identical behaviour. Hence, we plot only one representative for better readability. The SEY values of 2.6 and 2.7 are higher than for Nb. Moreover, the XPS data reveals a similar oxygen content as for the other samples. While the niobium oxides are reported with low SEY, the SEY of magnesium oxide, MgO, is between 4 and 10 which makes it a standard material for dynodes in photo muliplyers [16]. From this measurement it can therefore not be concluded if the high SEY is mainly due to hydrocarbons and water on the surface or from MgO. The chemical composition of the surfaces shows however a significant amount of oxygen as displayed in Figure 9. The Mg 2s peaks associated with MgO and MgB_2 could not be separated due to their overlap.

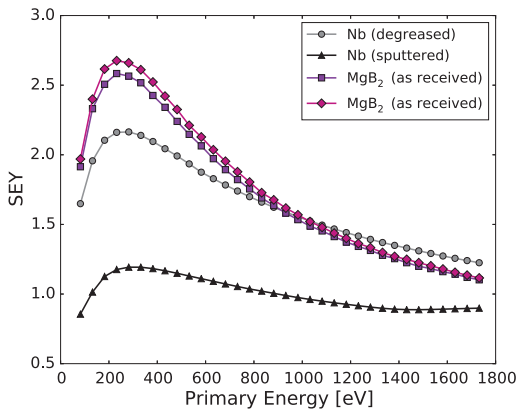

Figure 8: SEY of MgB_2

DISCUSSION AND CONCLUSION

The secondary electron yield is a crucial parameter to consider when exploring new materials for SRF applications. Since any SRF cavity will be exposed to air and water, SEY measurement need to be done on technical surfaces which are cleaned but account for the presence of hydrocarbons and native oxides on the surface.

The data from NbTiN, Nb_3Sn and Nb suggests that SRF cavities from niobium alloys should not suffer more from multipacting as bulk niobium cavities. However, it requires an RF test for definite confirmation. As the native niobium oxides, nitride and carbide are reported to have a low SEY, the measured SEY values as high as 2.5 are attributed to hydrocarbons and water on the surface.

The SEY found for the recently coated MgB_2 samples is slightly higher than for Nb_3Sn. Due to the reported very high SEY of MgO, the SEY of the MgB_2 samples can be attributed not only to hydrocarbons and water but also to the presence of MgO. MgB_2 is known to degrade under humidity resulting in the formation of MgO. An attempt of RF testing an MgB_2 sample in CERNs Quadrupole Resonator (QPR) failed due to heavy electron loading although great precautions were taken to minimize the exposure to air. After the RF test, the MgB_2 coating was visibly damaged in the high electric field regions as shown in Figure 10. It is worth mentioning that previous RF tests on MgB_2 in sample test cavities were able to measure the surface resistance but do not expose the sample to electric fields [17–19]. In terms of multipacting these measurements are therefore not representative to cavity operation.

In general, the presence of a significant amount of MgO makes a MgB_2 coating unsuitable for any RF exposed surface unless a passivation layer prevents the formation of MgO. A thickness of few nanometers is considered to be sufficient but the protection layer needs to have low RF power dissipation as it will be exposed and fully penetrated by the RF. The combination of low SEY and low RF losses is very restrictive to potential materials: Insulators have low (or no) RF losses but usually high SEY values. Metals have low SEY values but either a normal resistance or in case of superconductors, their critical field limits the maximum accelerating gradient.

ACKNOWLEDGMENT

We thank A.-M. Valente-Feliciano (JLab), S. Posen (Cornell), X.X. Xi (Temple U) and N. Valverde (CERN) for providing the samples for this study and C. Yung (STI) for providing the MgB_2 sample for the QPR test. This work is sponsored by the Wolfgang Gentner Programme of the German Federal Ministry of Education and Research (BMBF).

ISBN 978-3-95450-178-6

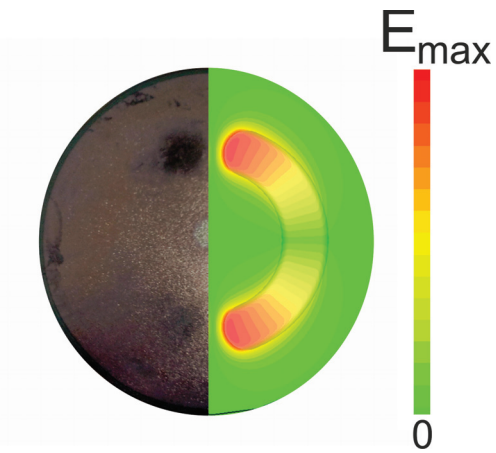

Figure 10: MgB_2 sample after the RF test with heavy electron loading. The right half indicates the electric field distribution on the sample.

REFERENCES

[1] C.M. Lyneis. Electron Loading - Description and Cures. In *Proceedings of the 1st Workshop on RF Superconductivity*, pages 119–144, Karlsruhe, Germany, July 1980.

[2] A. Shih, J. Yater, C. Hor, and R. Abrams. Secondary electron emission studies. *Applied Surface Science*, 111:251–258, 1997.

[3] H. Bruining. *Physics and Applications of Secondary Electron Emission*. Electronics and Waves – Pergamon Science Series. Pergamon Press LTD, London, UK, 1954.

[4] C. Scheuerlein and N. Hilleret. *The Influence of an Air Exposure on the Secondary Electron Yield of Copper*. Diplomarbeit, CERN-THESIS-2002-022, Geneva, Switzerland, 1997.

[5] V. Baglin, J. Bojko, C. Scheuerlein, O. Gröbner, M. Taborelli, B. Henrist, and N. Hilleret. The secondary electron yield of technical materials and its variation with surface treatments. In *Proceedings of the EPAC*, page 5, Vienna, Austria, 2000.

[6] N. Hilleret, C. Scheuerlein, and M. Taborelli. The secondary-electron yield of air-exposed metal surfaces. *Applied Physics A: Materials Science & Processing*, 76(7):1085–1091, May 2003.

[7] P. Ylä-Oijala. Electron multipacting in TESLA cavities and input couplers. *Part. Accel.*, 63:105–137, 1999.

[8] A.M. Valente-Feliciano, G. Eremeev, H.L. Phillips, C.E. Reece, J.K. Spradlin, Q. Yang, D. Batchelor, and R.A. Lukaszew. Nb(Ti)N based SIS multilayer strucutres for SRF applications. In *TUP088 SRF2013*, pages 664–667, Paris, France, 2013.

[9] M. Liepe and S. Posen. Nb3sn for SRF application. In *WEIA04 SRF2013*, pages 767–770, Paris, France, 2013.

[10] X.X. Xi, A.V. Pogrebnyakov, S.Y. Xu, K. Chen, Y. Cui, E.C. Maertz, C.G. Zhuang, Qi Li, D.R. Lamborn, J.M. Redwing, Z.K. Liu, A. Soukiassian, D.G. Schlom, X.J. Weng, E.C. Dickey, Y.B. Chen, W. Tian, X.Q. Pan, S.A. Cybart, and R.C. Dynes. MgB2 thin films by hybrid physical chemical vapor deposition. *Physica C: Superconductivity*, 456(1-2), June 2007.

[11] R. Calder, G. Dominichini, and N. Hilleret. Influence of various vacuum surface treatments on the secondary electron yield of niobium. *Nuclear Instruments and Methods in Physics Research Section B: Beam Interactions with Materials and Atoms*, 13(1-3):631–636, March 1986.

[12] R. Warnecke. Émission secondaire de métaux purs. *Journal de Physique et le Radium*, 7(6):270–280, 1936.

[13] E.L. Garwin, E.W. Hoyt, R.E. Kirby, and T. Momose. Secondary electron yield and Auger electron spectroscopy measurements on oxides, carbide, and nitride of niobium. *Journal of Applied Physics*, 59(9):3245, 1986.

[14] H. Seiler. Secondary electron emission in the scanning electron microscope. *Journal of Applied Physics*, 54(11), 1983.

[15] J.N. Miller, I. Lindau, and W.E. Spicer. A photoemission study of clean and oxidized Nb3Sn. *Physics Letters A*, 88(2):97–99, February 1982.

[16] G.F. Knoll. *Radiation detection and measurement*. Wiley, New York, 3rd ed edition, 2000.

[17] D.E. Oates, Y.D. Agassi, and B.H. Moeckly. Microwave measurements of MgB2: implications for applications and order-parameter symmetry. *Superconductor Science and Technology*, 23(3):034011, March 2010.

[18] T. Tajima, L. Civale, N.F. Haberkorn, R.K. Schulze, V.A. Dolgashev, J. Guo, D.W. Martin, S.G. Tantawi, C. Yoneda, H. Inoue, A. Matsumoto, E. Watanabe, B.H. Moeckly, C. Yung, M.J. Pellin, T. Proslier, X Xi, and B. P. Xiao. MgB2 Thin Film Studies. In *Proceedings of the 15th Conference on RF Superconductivity*, page 287, Chicago, USA, 2011.

[19] B.P. Xiao, X. Zhao, J. Spardlin, C.R. Reece, M.J. Kelley, T. Tan, and X.X. Xi. Surface Impedance Measurements of Single Crystal MgB2 Films for Radiofrequency Superconductivity Applications. *Superconductor Science and Technology*, 25:095006, 2012.